

UC Davis

UC Davis Previously Published Works

Title

Mechanisms of Reduced Astrocyte Surface Coverage in Cortical Neuron-Glia Co-cultures on Nanoporous Gold Surfaces

Permalink

<https://escholarship.org/uc/item/7t9393p2>

Journal

Cellular and Molecular Bioengineering, 9(3)

ISSN

1865-5025

Authors

Chapman, CAR
Chen, H
Stamou, M
[et al.](#)

Publication Date

2016-09-01

DOI

10.1007/s12195-016-0449-4

Peer reviewed

Cellular and Molecular Bioengineering



2016 CMBE Young Innovators Special Issue

Editors: T.A. Desai and M.R. King

A Journal of the Biomedical Engineering Society



Mechanisms of Reduced Astrocyte Surface Coverage in Cortical Neuron-Glia Co-cultures on Nanoporous Gold Surfaces

Christopher A. R. Chapman¹, Hao Chen², Marianna Stamou^{2,#}, Pamela J. Lein², Erkin Seker^{3*}

¹Department of Biomedical Engineering, ²Department of Molecular Biosciences, and ³Department of

Electrical and Computer Engineering

University of California - Davis, Davis, California 95616, United States

Current Affiliation: [#]Department of Health Sciences and Technology, Swiss Federal Institute of Technology (ETH) Zurich, Zurich, Switzerland

*Corresponding Author: Prof. Erkin Seker

Address: 3177 Kemper Hall, Dept. of Electrical and Computer Engineering, UC Davis, CA 95616

Email: eseker@ucdavis.edu

Phone: 530-752-7300

Fax: 530-752-8428

Abstract

Nanoporous gold (np-Au) is a promising multifunctional material for neural electrodes. We have previously shown that np-Au nanotopography reduces astrocyte surface coverage (linked to undesirable gliosis) while maintaining high neuronal coverage in a cortical primary neuron-glia co-culture model as long as two weeks *in vitro*. Here, we investigate the potential influence of secreted soluble factors from cells grown on np-Au on the cell type-specific surface coverage of cells grown on conventional tissue culture plastic and test the hypothesis that secretion of factors is responsible for inhibiting astrocyte coverage on np-Au. In order to assess whether factors secreted from cells grown on np-Au surfaces reduced surface coverage by astrocytes, we seeded fresh primary rat neuron-glia co-cultures on conventional polystyrene culture dishes, but maintained the cells in conditioned media from co-cultures grown on np-Au surfaces. After one week *in vitro*, a preferential reduction in astrocyte surface coverage was not observed, suggesting that soluble factors are not playing a role. In contrast, four hours after cell seeding there were a significant number of non-adhered, yet still viable, cells for the cultures on np-Au surfaces. We hypothesize that the non-adherent cells are mainly astrocytes, because: (i) there was no difference in neuronal cell coverage between np-Au and pl-Au for long culture durations and (ii) neurons are post-mitotic and not expected to increase in number upon attaching to the surface. Overall, the results suggest that the np-Au topography leads to preferential neuronal attachment shortly after cell seeding and limits astrocyte-specific np-Au surface coverage at longer culture durations.

Key Terms: nanostructure, cell-material interaction, nanoporous gold, soluble factors, cell attachment, neuron-glia co-culture, neuroengineering, gliosis

Biography

Dr. Erkin Şeker joined the Department of Electrical and Computer Engineering at UC Davis in 2011. He received his PhD degree in Electrical Engineering from the University of Virginia (UVA) in 2007, where he developed techniques to control mechanical and morphological properties of nanoporous gold. During his postdoctoral appointment in the Department of Chemistry at UVA he investigated material-biomolecule interactions and developed microfluidic flow control schemes. Between 2009 and 2011, as a research associate at the Center for Engineering in Medicine at Harvard Medical School, he developed multiple electrode arrays for neural electrophysiology applications and spearheaded the development of microsystems for monitoring transcriptional and secretory dynamics at a cellular-level in the context of metabolic dysregulation. At UC Davis, he is leading the interdisciplinary Multifunctional Nanoporous Metals research group with the overarching goal of understanding and controlling nanostructured material properties and their interaction with biological systems to develop effective biomedical tools for both basic and clinical applications. He is the recipient of Fund for Medical Discovery Award from Massachusetts General Hospital and a NSF CAREER Award. He served as an Associate Scientific Advisor for Science Translational Medicine journal and was selected to participate in National Academy of Engineering's Annual Frontiers of Engineering Education Symposium in 2014.

Introduction

Nanostructured materials with properties unique to the nanoscale have shown substantial promise as multifunctional coatings in a myriad of biointerfaces, ranging from orthopedic implants to neural electrodes.^{15, 20, 27, 33} For example, the large effective surface area of nanostructured sensor coatings reduces impedance of neural interfaces for higher fidelity electrophysiological recordings,²⁸ nanotubular structures allow for higher loading capacity and sustained delivery of pharmaceuticals,^{16, 21} and nanopores act as size-selective sieves to enhance the performance of electrochemical DNA sensors in the presence of globular biofouling proteins.^{7, 25} In addition to these attributes, micro- and nano-topographical cues from nanostructured materials have been shown to guide cell growth, phenotype, and differentiation across many cell types, which are important factors for interfaces where specific cell coupling is beneficial.^{3, 4, 8, 13, 14} One emerging material that has shown promise in promoting specific cell coupling is nanoporous gold (np-Au). Np-Au is a nanostructured material that is produced by selective dissolution of silver from a gold-silver alloy, resulting in a network of gold ligaments and pores.^{11, 31} Specifically, np-Au has attracted attention for its applications in electrochemical sensors,^{12, 22, 29} catalytic platforms,¹⁸ fundamental nanoscale materials studies,^{6, 10} tunable drug release,²¹ and high fidelity recordings from organotypic brain slices.³⁰ These properties, along with its compatibility with microfabrication techniques, suggest np-Au as an attractive option for high sensitivity multifunctional biosensors with potential applications ranging from lab-on-a-chip based field devices to implantable drug-eluting neural electrodes. We have previously shown that np-Au nanotopography reduces the ability of astrocytes to spread across the surface, while maintaining high neuronal coverage as long as two weeks *in vitro* in a cortical primary neuron-glia co-culture model.⁵ Additionally, we have shown that np-Au does not alter the proliferation rate of astrocytes and therefore reduces only the hypertrophic cell surface coverage that is partially responsible for undesirable gliosis.^{26, 36} Here, we investigate the potential influence of secreted soluble factors on the cell type-specific surface coverage as well as the initiation of this phenomenon at earlier time points after plating. Specifically, the working hypotheses are: (i) soluble factors secreted from cells on np-Au surfaces, in response to the material nanostructure, inhibit the ability for astrocytes to spread across the np-Au surface; and (ii) reduced adhesion

of astrocytes onto the np-Au surface within four hours of cell plating translates into reduced surface coverage by astrocytes at longer times in culture.

Materials & Methods

2.1 Sample fabrication and characterization: Samples were typically deposited in 5 mm-diameter spots onto the middle of a piranha-cleaned 12 mm-diameter thin (0.15 mm-thick) glass slide. Unstructured planar gold (pl-Au) samples were deposited by direct current sputtering (Kurt J. Lesker) of a 200 nm-thick gold layer (at 10 mTorr argon) on top of the substrate coated with a 160 nm-thick chromium adhesion layer. Gold-silver alloy spots (precursor to np-Au) were fabricated by sputtering a 160 nm-thick chromium adhesion layer, 80 nm-thick gold corrosion barrier layer, and a 600 nm-thick gold and silver alloy (64% silver and 36% gold; atomic %). The final np-Au films were fabricated by immersing the gold-silver alloy in heated (55°C) nitric acid (70%) for 15 minutes. The short dealloying times used in the present study typically result in residual silver levels in the order of 3-5 atomic percent.⁵ The samples were then soaked in deionized (DI) water for one week while replacing the water every 24 hours. In order to produce both a high silver content np-Au film with similar feature sizes and np-Au films with increased feature sizes, the nitric acid concentration was decreased to 50% with dealloying times ranging from 10 minutes to 24 hours.

Caution: Nitric acid is highly corrosive and reactive with organic materials and must be handled with extreme care. The morphology of the coatings was characterized by scanning electron microscopy (FEI Nova NanoSEM430), and elemental compositions before and after dealloying were assessed with energy dispersive X-ray spectroscopy (Oxford INCA, EDS).

2.2 Primary cortical neuron-glia mixed culture: Primary rat cortical cells were obtained from the laboratory of Prof. Pamela J. Lein at the University of California, Davis. All studies were conducted according to protocols approved by the Institutional Animal Care and Use Committee of the University of California, Davis. Surface samples were incubated with 0.5 mg/mL poly-L-lysine in B Buffer (boric acid and borax, Sigma, Saint Louis, MO) at 37°C in 5% CO₂ for 4 hours. The samples were then washed with sterile deionized (DI) water and incubated for 12 hours at 37°C and 5% CO₂ with plating media consisting of 2%

B27 supplement, 1X Glutamax, 10% heat-inactivated horse serum, and 1M HEPES at pH 7.5 with Neurobasal A as the basal medium (all media components were obtained from Invitrogen, Carlsbad, CA). Dissociated cortical cells were seeded in plating medium at a density of 50,000 cells/cm² on each material, allowed to adhere for 4 hours, and switched to serum-free growth medium. At day *in vitro* (DIV) 4 and at DIV 7 cell culture medium was replenished by adding fresh growth medium.

2.3 Primary cortical astrocyte culture: Primary rat cortical cells were obtained as previously described above. At DIV 1 the cell cultures were mechanically agitated to detach neurons from the surface of the tissue culture flask. The resulting ‘purified’ astrocyte culture was maintained and passaged for 7 days *in vitro* before being plated onto substrates at a density of 50,000 cells/cm². Purified astrocyte cultures were maintained in a DMEM based media containing Earle’s salts, 10% fetal bovine serum, and 5% penicillin/streptomycin (Invitrogen, Carlsbad, CA).

2.4 Conditioned media experimental protocol: Primary rat cortical cells were seeded onto both np-Au and pl-Au samples at a density of 50,000 cells/cm². Cultures were maintained on these samples for 1, 7, and 12 days respectively replenishing and changing media as per the protocol outlined above. The media from these cultures grown on np-Au and pl-Au was collected at the designated day (i.e. day *in vitro* 1, 7, and 12) before the cultures were fixed. The collected media from each of these experiments was then used to grow fresh cultures that were plated onto conventional polystyrene tissue culture plastic at a density of 50,000 cells/cm². These cultures were grown to day *in vitro* (DIV) 7. This resulted in six different conditions being tested: conditioned media from cells cultured on np-Au surfaces to DIV 1, 7, and 12, as well as conditioned media from cells cultured on pl-Au surfaces to DIV 1, 7, and 12 (Figure 1). Additionally, as a control parameter non-conditioned (fresh) medium was also used to grow newly plated cultures on polystyrene surfaces to DIV 7. All cultures were fixed at their designated time with 4% paraformaldehyde in phosphate buffered saline (Affymetrix), and immunostained using mouse anti-tubulin- β III antibodies (Invitrogen) to identify neurons, and rabbit anti-gial fibrillary acidic protein antibodies (GFAP, Invitrogen) to identify

astrocytes, followed by incubation with goat anti-mouse antibodies conjugated to Alexa Fluor 555 (Invitrogen) and goat anti-rabbit antibodies conjugated to Alexa Fluor 488 (Invitrogen) all at a concentration of 1:100. Counter-staining with DAPI was used to visualize cell nuclei. Images of immunostained samples were acquired using an inverted fluorescent microscope (Zeiss Observer D1). Sample sizes of at least three images (10X magnification – 895 μm x 671 μm) per experimental parameter were captured and subsequently analyzed using a custom ImageJ macro to determine the total cell coverage on a given surface.

2.5 Initial cell attachment experimental protocol: Primary rat cortical cells were plated onto surfaces consisting of np-Au, pl-Au, precursor alloy, and glass at a density of 50,000 cells/cm². Cultures were given four hours to adhere to each surface before the non-adherent cells were collected by extracting the medium from each sample (Figure 2). This solution of non-adherent cells was then analyzed for cell density (number of cells) and viability through a trypan blue exclusion (ThermoFisher Scientific) test in conjunction with a hemocytometer (Brightline). This protocol was then repeated using only a purified primary astrocyte culture plated at the same density.

2.6 Statistical methods: Each study was performed on at least three different samples per dissection, and imaged at the same five locations on each sample. Unless otherwise stated, the reported values represent averages of all samples in an experimental group and standard deviations of the measurements. A two-tailed Student's t-test assuming unequal variance was used to identify differences between two different sample groups and a one-way ANOVA was used when comparing more than two groups in each experiment. p-values less than 0.05 were deemed statistically significant.

Results and Discussion

The material of focus in this study, nanoporous gold (np-Au), is obtained through a *dealloying* process, where silver atoms are removed from the alloy and gold atoms undergo surface diffusion creating an interconnected network of ligaments and pores. The resulting network presents a typical porosity of

approximately 70% with a median ligament size of approximately 30 nm, and non-cytotoxic levels of residual silver at 3-5 atomic percent (Figure 3).⁵ In a previous study we have demonstrated that the np-Au surface morphology, and not residual silver, results in reduced astrocyte (but not neuronal) surface coverage at DIV 7 and 12.⁵ However, the extent to which soluble factors influence cell surface coverage in the long-term as well as the short-term initiation of this phenomenon are not known. Therefore, the goal of experiments here are to determine the contribution of secreted factors to this long term reduction in astrocyte surface coverage as well as to determine the initial adhesive response of astrocytes to the surface of np-Au.

3.1 Investigating the role of cell secreted factors on the reduction in astrocyte coverage on np-Au

Although there is strong evidence that the nanostructure of np-Au plays a dominant effect in the reduction of astrocyte surface coverage, it is unclear whether the topographical cues directly influence spreading of astrocytes or whether factors secreted by cells cultured on np-Au influence astrocyte spreading via an autocrine/paracrine signaling mechanism. Soluble cell secreted factors from neurons, astrocytes, and other glia are known to influence astrocyte surface coverage and morphology. Most notably, neurons secrete many fibroblast growth factors and glia secrete many pro-inflammatory factors such as tumor necrosis factor alpha, interleukin-6, all of which can effect astrocyte morphology and cause an increase in cell reactivity.^{1, 19, 32, 35} Additionally, soluble factors from neural slice cultures have been shown to induce glioma cell proliferation.³⁴ Given the potential influence of soluble factors in the cell type-specific reduction of astrocyte surface coverage, we test the first hypothesis concerning the role of secreted factors in reduced astrocyte coverage on np-Au. In order to test this hypothesis, conditioned culture media from cortical cultures grown on np-Au and pl-Au was collected on DIV 1, DIV 7 and DIV 12. The conditioned media was then used to culture freshly harvested cortical cells on conventional polystyrene tissue culture plastic for 7 days (illustrated in Figure 1). This experimental design ensures that the influence of soluble factors and topographical cues are decoupled.

At DIV 7, the time point at which a clear reduction in astrocyte surface coverage becomes apparent in cultures on np-Au,⁵ cortical cultures grown on tissue culture plastic were immunostained with markers for

neurons and astrocytes to quantify cell type-specific surface coverage in response to the different conditioned media (Figure 4). The neuronal surface coverage remained similar (all samples ANOVA $p = 0.3$) on polystyrene surfaces whether the culture was maintained in fresh (un-conditioned) medium or conditioned medium from np-Au or pl-Au cultures (Figure 5A). In contrast, the astrocyte surface coverage monotonically increased in response to the conditioned medium from DIV 1, 7, and 12 cultures grown on np-Au and pl-Au (Figure 5B). These results suggest that the accumulation of soluble factors in conditioned media enhance proliferation and/or the spreading of astrocytes. More importantly, a pair-wise comparison between conditioned media from np-Au and pl-Au for astrocyte surface coverage in cultures on polystyrene surface at DIV 7 and 12 did not reveal significant differences. This suggests that when the topographical cues are removed (which is the case of cells grown on polystyrene with conditioned media), the astrocyte-specific reduction in surface coverage is no longer present. To complement this observation, we compared the surface coverage of neurons and astrocytes on the samples (np-Au and pl-Au) that were used for preparing the conditioned media. A clear reduction in astrocyte surface coverage was seen on np-Au at DIV 7 and 12 (Figure 5D), while the neuronal coverage remained unchanged (Figure 5C). Additionally, visual comparison between high magnification images of neurons and astrocytes at DIV 12 (Figure 6) demonstrate that clear differences in astrocyte morphology arise in response to the material surface, an effect that is not seen between conditioned media samples. Astrocyte morphologies on np-Au typically consist of fewer processes, often losing their typical 'star-shaped' cell morphology. Further studies are underway to determine whether np-Au topography contributes to this morphological difference by affecting the local formation of focal adhesions.

3.2 Effects of np-Au surface morphology on initial astrocyte attachment

To test the second hypothesis of whether initial cellular adhesion upon seeding dictates long-term reduction in cellular coverage, we quantified non-adherent cells and their viability in cultures grown on np-Au, pl-Au, precursor alloy, and glass. Non-adherent cells were quantified in media collected from each sample four hours after cell seeding (illustrated in Figure 2). As shown in Figure 7, np-Au reduces the ability of cortical cells to adhere in comparison to all surfaces. An approximately 2.4-fold increase in viable non-

adherent cells ($p < 0.005$) was seen in the medium aspirated from np-Au samples in comparison to medium from pl-Au samples (Figure 7A). Although the np-Au surface led to an increase in the number of viable non-adherent cells, there was no change in the number of dead non-adherent cells in the aspirated medium in comparison to either pl-Au or glass. On the other hand, the silver-rich cytotoxic precursor alloy significantly increased the number of dead non-adherent cells ($p < 0.01$) in comparison to all other materials tested. This result, taken together with the results of the previous study that showed no change in astrocyte proliferation rates,⁵ suggests that np-Au is causing an initial reduction in cortical cell adhesion via non-cytotoxic mechanisms. However, it is still unclear whether it is astrocytes or neurons that are affected by this reduction in initial cellular adhesion. To investigate the effect of surface coating on specifically the astrocytes, the cell adhesion experiments were repeated using purified astrocyte cultures from primary rat cortical cells. The number of viable non-adherent astrocytes four hours after plating for the np-Au sample was twice ($p < 0.01$) that for pl-Au (Figure 7B). Given a similar fold-increase in non-adherent cell number of cortical cells, this result suggests that the np-Au surface is non-permissive to astrocyte attachment. Surprisingly, this reduction in the initial attachment of astrocytes on np-Au does not seem to alter density or proliferation of astrocytes at later time points in culture, as previously published.⁵ These results suggest that the decreased cellular attachment to the np-Au surface is likely due to the complex nanotopography of the np-Au surface limiting adhesion sites. Additionally, astrocytes appear less likely than neurons to attach to this nanostructured surface. This can potentially be attributed to differences in focal adhesion size between astrocytes and neurons.² It is likely that this probabilistic cell-surface interaction plays a similar role in sustained reduction in astrocyte surface coverage on np-Au surfaces at longer time-points (past DIV 7).

Conclusions

We have decoupled putative influences of topographical and soluble cues to reveal that astrocyte-specific reduction in surface coverage on np-Au surfaces is due to both an initial inhibition of astrocyte attachment and topographical cues provided by the np-Au nanostructure. At early time points (4 hours) after seeding, the reduction in astrocyte adhesion on np-Au compared to pl-Au surface can be attributed to kinetically-

determined focal adhesion establishment during probabilistic interactions between the cellular adhesive molecules and the complex nanotopography (composed of voids and ligaments) of the np-Au surface.^{9, 23} For later time points, when the reduced astrocyte surface coverage on np-Au persists, the phenomenon can at least be partially attributed to the mechanical inhibition of focal adhesion complexes;^{5, 14, 17} however, it is also possible that the cell response is in part mediated via mechanotransduction by the np-Au topography through signaling pathways (such as YAP/TAZ²⁴) or other integrin-mediated pathways.^{3, 8} Further research is underway to identify the focal adhesion complex formation efficiency of astrocytes as a function of np-Au feature size. Ultimately, the results presented here demonstrate an advancement in understanding of the cellular mechanisms leading to the reduced astrocyte surface coverage on np-Au films compared to planar materials and conventional polystyrene.

Acknowledgements

We gratefully acknowledge support from UC Lab Fees Research Program Award [12-LR-237197], Research Investments in the Sciences & Engineering (RISE) Award, and National Science Foundation Awards (CBET-1512745 and CBET&DMR-1454426). C. Chapman was supported by a National Science Foundation Graduate Research Fellowship [DGE-1148897] and a predoctoral fellowship from the National Institute of Health [T32-GM008799]. Support was also provided by the CounterACT Program, National Institutes of Health Office of the Director, and the National Institutes of Neurological Disorders and Stroke [U54-NS079202]. H. Chen was supported by a predoctoral fellowship from the National Institute of Environmental Health Sciences [T32-ES007059]. H. Chen and M. Stamou received predoctoral fellowships from the UC Davis Superfund Basic Research Program [P42-ES04699].

Conflicts of Interest

E. Seker has an issued patent, titled "Nanoporous metal multiple electrode array and method of making same". C. A. R. Chapman, H. Chen, M. Stamou, and P. J. Lein declare that they have no conflicts of interest.

Ethical Standards

All studies were conducted according to protocols approved by the Institutional Animal Care and Use Committee of the University of California, Davis. No human subjects research was performed in this study.

References

1. Agarwal, A.; Bergles, D. E. Astrocyte morphology is controlled by neuron-derived FGF. *Neuron* 83:255-257, 2014.
2. Arregui, C.; Carbonetto, S.; McKerracher, L. Characterization of neural cell adhesion sites: point contacts are the sites of interaction between integrins and the cytoskeleton in PC12 cells. *J. Neurosci.* 14:6967-6977, 1994.
3. Biggs, M. J. P., Richards, R. G. & Dalby, M. J. Nanotopographical modification: a regulator of cellular function through focal adhesions. *Nanomedicine* 6:619-633, 2010.
4. Blumenthal, N. R., Hermanson, O., Heimrich, B. & Shastri, V. P. Stochastic nanoroughness modulates neuron-astrocyte interactions and function via mechanosensing cation channels. *P. Natl. A. Sci.* 111:16124-16129, 2014.
5. Chapman, C. A. R., Chen, H., Stamou, M., Biener, J., Biener, M. M., Lein, P. J. & Seker, E. Nanoporous gold as a neural interface coating: effects of topography, surface chemistry, and feature size. *ACS Appl. Mater. Interfaces* 7:7093-7100, 2015.
6. Chapman, C. A. R., Daggumati, P., Gott, S. C., Rao, M. P. & Seker, E. Substrate topography guides pore morphology evolution in nanoporous gold thin films. *Scripta Mater.* 110:33-36, 2016.
7. Daggumati, P., Matharu, Z., Wang, L. & Seker, E. Biofouling-resilient nanoporous gold electrodes for DNA sensing. *Anal. Chem.* 87:8618-8622, 2015.
8. Dalby, M. J., Gadegaard, N. & Oreffo, R. O. C. Harnessing nanotopography and integrin-matrix interactions to influence stem cell fate. *Nat. Mater.* 13:558-569, 2014.
9. Dembo, M.; Torney, D.; Saxman, K.; Hammer, D. The reaction-limited kinetics of membrane-to-surface adhesion and detachment. *Proc. R. Soc. Lond., Ser. B: Biol. Sci.* 234:55-83, 1988.
10. Dorofeeva, T. S. S., E. Electrically-tunable pore morphology in nanoporous gold thin films. *Nano Res.*, 2015.
11. Erlebacher, J., Aziz, M. J., Karma, A., Dimitrov, N. & Sieradzki, K. Evolution of nanoporosity in dealloying. *Nature* 410:450-453, 2001.

12. Feng, J., Zhao, W. & Wu, J. A label-free optical sensor based on nanoporous gold arrays for the detection of oligodeoxynucleotides. *Biosens. Bioelectron.* 30:21-27, 2011.
13. Gasiorowski, J. Z., Liliensiek, S. J., Russel, P., Stephan, D. A., Nealey, P. A. & Murphy C. J. Alterations in Gene Expression of Human Vascular Endothelial Cells Associated with Nanotopographic Cues. *Biomaterials* 31:8882-8888, 2010.
14. Geiger, B.; Spatz, J. P.; Bershadsky, A. D. Environmental sensing through focal adhesions. *Nat. Rev. Mol. Cell Bio.* 10:21-33, 2009.
15. Goldberg, M., Langer, R. & Jia, X. Nanostructured materials for applications in drug delivery and tissue engineering. *J. Biomater. Sci., Polym. Ed.* 18:241-268, 2007.
16. Gultepe, E.; Nagesha, D.; Sridhar, S.; Amiji, M. Nanoporous inorganic membranes or coatings for sustained drug delivery in implantable devices. *Adv. Drug Del. Rev.* 62:305-315, 2010.
17. Jeon, H.; Koo, S.; Reese, W. M.; Loskill, P.; Grigoropoulos, C. P.; Healy, K. E. Directing cell migration and organization via nanocrater-patterned cell-repellent interfaces. *Nat. Mater.* 14:918-923, 2015.
18. Jin, H. J. W., J. A material with electrically tunable strength and flow stress. *Science* 332:1179-1182, 2011.
19. Kang, K., Lee, S., Han, J. E., Choi, J. W. & Song, M. The complex morphology of reactive astrocytes controlled by fibroblast growth factor signaling. *Glia* 62:1328-1344, 2014.
20. Kotov, N. A., Winter, J. O., Clements, I. P., Jan, E., Timko, B. P., Campidelli, S., Pathak, S., Mazzatenta, A., Lieber, C. M., Prato, M., Bellamkonda, R. V., Silva, G. A., Kam, N. W. S., Patolsky, F. & Ballerini, L. Nanomaterials for neural interfaces. *Adv. Mater.* 21:3970-4004, 2009.
21. Kurtulus, O., Daggumati, P. & Seker, E. Molecular release from patterned nanoporous gold thin films. *Nanoscale* 6:7062-7071, 2014.
22. Li, K., Huang, J., Shi, G., Zhang, W. & Jin, L. A sensitive nanoporous gold-based electrochemical DNA biosensor for *Escherichia coli* detection. *Anal. Lett.* 44:2559-2570, 2011.

23. Mody, N. A.; King, M. R. Influence of Brownian motion on blood platelet flow behavior and adhesive dynamics near a planar wall. *Langmuir* 23:6321-6328, 2007.
24. Morgan, J. T., Murphy, C. J. & Russell, P. What do mechanotransduction, Hippo, Wnt, and TGFB have in common? YAP and TAZ as key orchestrating molecules in ocular health and disease. *Exp. Eye Res.* 115:1-12, 2013.
25. Patel, J., Radhakrishnan, L., Zhao, B., Uppalapati, B., Daniels, R.C., Ward, K.R. & Collinson M.M. Electrochemical properties of nanostructured porous gold electrodes in biofouling solutions. *Anal. Chem.* 85:11610-11618, 2013.
26. Polikov, V. S., Tresco, P.A. & Reichert, W.M. Response of brain tissue to chronically implanted neural electrodes. *J. Neurosci. Methods* 148:1-18, 2005.
27. Popat, K. C.; Leoni, L.; Grimes, C. A.; Desai, T. A. Influence of engineered titania nanotubular surfaces on bone cells. *Biomaterials* 28:3188-3197, 2007.
28. Robinson, D. A. The electrical properties of metal microelectrodes. *Proc. IEEE* 56:1065-1071, 1968.
29. Santos, G. M., Zhao, F., Zeng, J. & Shih, W. Characterization of nanoporous gold disks for photothermal light harvesting and light-gated molecular release. *Nanoscale* 6:5718-5724, 2014.
30. Seker, E., Berdichevsky, Y., Begley, M.R., Reed, M.L., Staley, K.J. & Yarmush, M.L. The fabrication of low-impedance nanoporous gold multiple-electrode arrays for neural electrophysiology studies. *Nanotechnology* 21:1-7, 2010.
31. Seker, E., Reed, M. L. & Begley, M. R. Nanoporous gold: fabrication, characterization, and applications. *Materials* 2:2188-2215, 2009.
32. Sofroniew, M. V. V., H. V. Astrocytes: biology and pathology. *Acta Neuropathol.* 119:7-35, 2010.
33. Solanki, P. R., Kaushik, A., Agrawal, V. V. & Malhotra, B. D. Nanostructured metal oxide-based biosensors. *NPG Asia Mater.* 3:17-24, 2010.
34. Venkatesh, H. S., Johung, T. B., Caretti, V., Noll, A., Tang, Y., Nagaraja, S., Gibson, E. M., Mount, C. W., Polepalli, J., Mitra, S. S., Woo, P. J., Malenka, R. C., Vogel, H., Bredel, M., Mallick, P. &

- Monje, M. Neuronal activity promotes glioma growth through neuroligin-3 secretion. *Cell* 161:803-816, 2015.
35. Wagoner, N. J., Oh, J., Repovic, P. & Benveniste, E. N. Interleukin-6 production by astrocytes: autocrine regulation by IL-6 and the soluble IL-6 receptor. *J. Neurosci.* 19:5236-5244, 1999.
36. Woolley, A. J., Desai, H. A. & Otto K. J. Chronic intracortical microelectrode arrays induce non-uniform, depth-related tissue responses. *J. Neural Eng.* 10:1-11, 2013.

Figure Legends

Figure 1 (Christopher Chapman) – Neuron-glia co-cultures were plated on samples of np-Au and pl-Au.

These cultures were grown to day 1, 7, and 12 *in vitro* respectively. The conditioned media from these cultures were then used to maintain neuron-glia co-cultures on conventional polystyrene tissue culture surfaces for 7 days.

Figure 2 (Christopher Chapman) – Neuron-glia co-cultures were plated on samples of np-Au, pl-Au, glass, and precursor Au-Ag alloy. After allowing four hours for cell attachment, non-adherent cell number and viability were quantified by a trypan blue exclusion test.

Figure 3 (Christopher Chapman) – (A) A low magnification (50,000X) scanning electron micrograph of nanoporous gold (np-Au) showing the long range uniformity of the ligament network. (B) A high magnification (200,000X) scanning electron micrograph of np-Au showing detail of ligaments and pores. (C) A high magnification (200,000X) scanning electron micrograph of planar gold (pl-Au) showing a clear granular surface structure.

Figure 4 (Christopher Chapman) – Fluorescent micrographs of cortical neurons (red – Tubulin- β III), astrocytes (green – GFAP), and cell nuclei (blue – DAPI) grown on tissue culture plastic (polystyrene) for seven days *in vitro* using conditioned media from cortical cells grown on np-Au and pl-Au samples at (A) DIV 1, (B) 7, and (C) 12 as well as (D) with un-conditioned fresh media.

Figure 5 (Christopher Chapman) – (A) Rat cortical cells were seeded on conventional culture plastic and maintained for 7 days in conditioned media from DIV 1 or DIV 7 or DIV 12 cortical cells which had been grown on np-Au or pl-Au surfaces. Plastic surface coverage by neurons on DIV 7 is not affected by the composition/age of the conditioned media ($p = 0.8$). (B) Astrocyte surface coverage at DIV 7 on polystyrene only exhibits significant increase between cultures grown with increasing age of the conditioned media

from both np-Au and pl-Au ($p < 0.05$), with no effect of the conditioning substrate. (C) Neuron surface coverage on np-Au and pl-Au samples at DIV 1, 7, and 12 is not different between the two sample surfaces. (D) Sustained decrease in np-Au surface coverage by astrocytes at DIV 1, 7, and 12 compared to astrocytes grown on pl-Au.

Figure 6 (Christopher Chapman) – High magnification fluorescent micrographs of neurons (red – Tubulin- β III), astrocytes (green – GFAP), and cell nuclei (blue – DAPI) grown to day *in vitro* 12 on (A) np-Au and (B) pl-Au.

Figure 7 (Christopher Chapman) – (A) A 2.4-fold increase in the number of live non-adherent cells from the np-Au surface ($p < 0.005$) in comparison to non-structured pl-Au and glass samples suggest that the np-Au topography reduced cell attachment via non-cytotoxic mechanisms. (B) A 2-fold increase in the number of live non-adherent astrocytes ($p < 0.01$) on the surface of np-Au suggests that astrocytes are the dominant cell-type in the non-adherent cortical cells.

Figures

Figure 1 (Christopher Chapman)

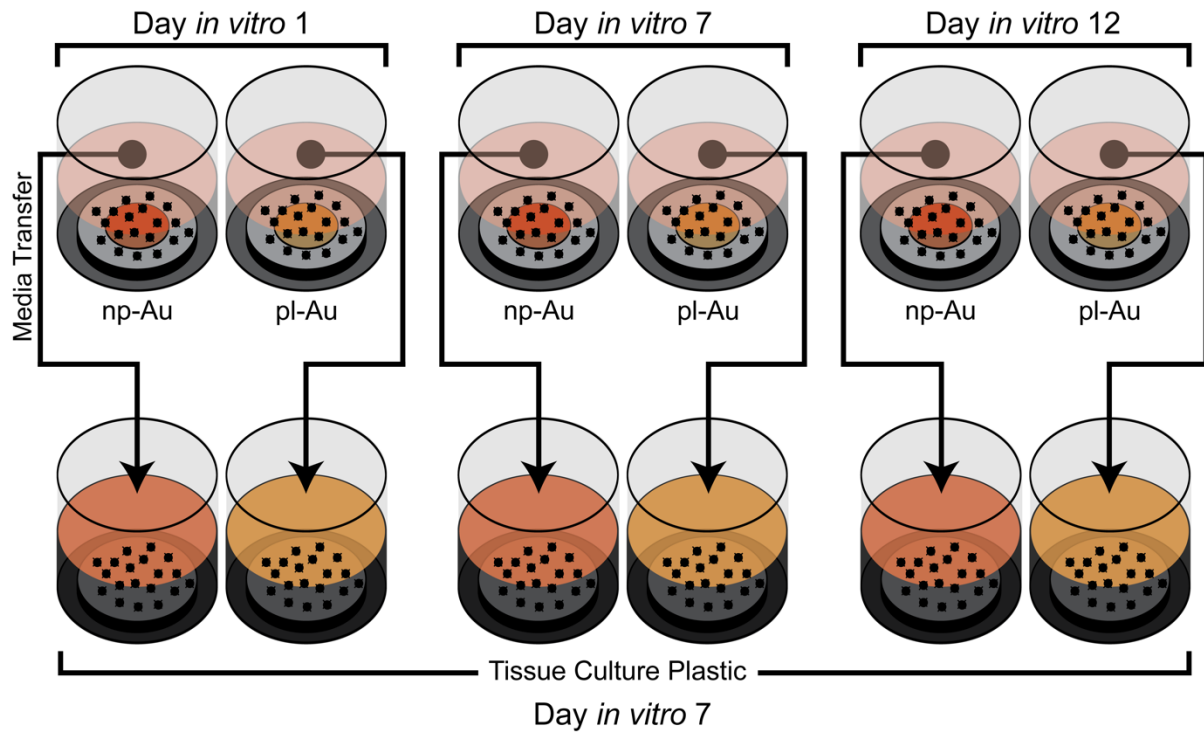


Figure 2 (Christopher Chapman)

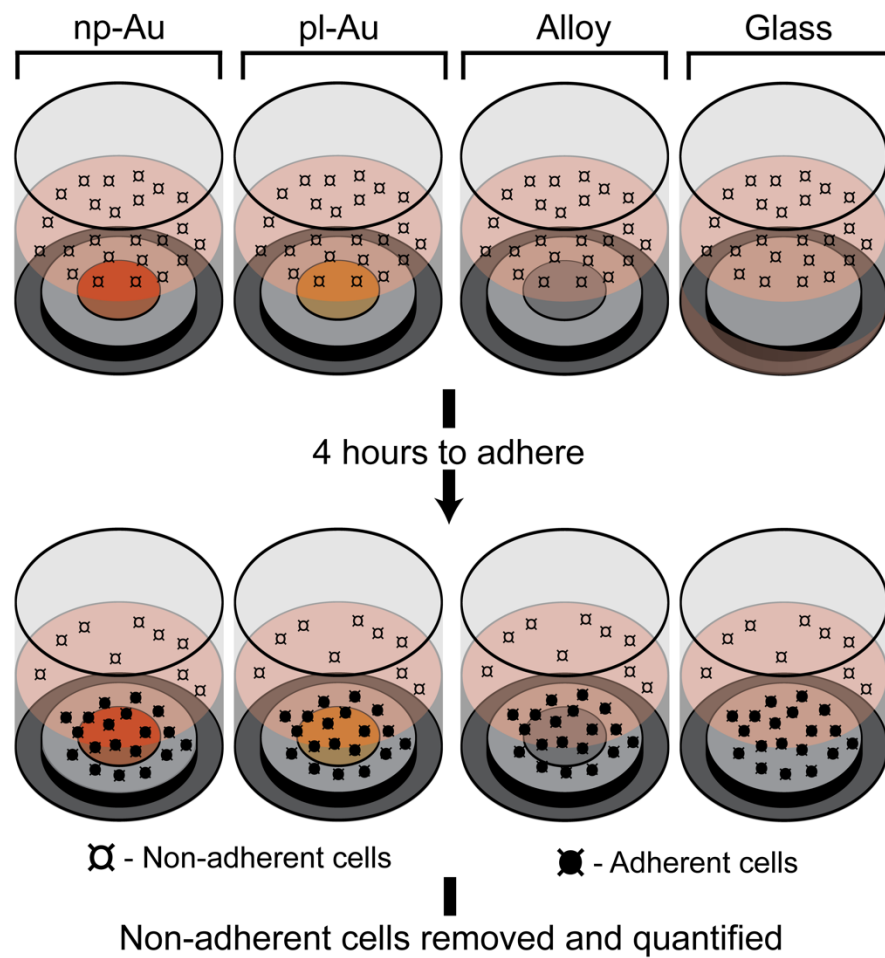
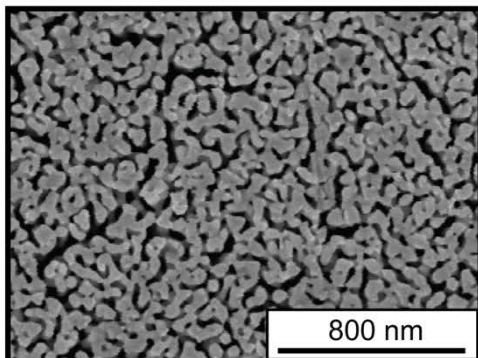
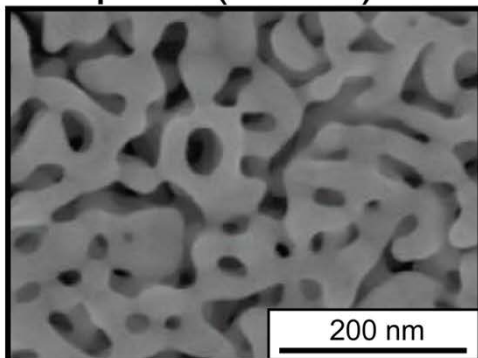


Figure 3 (Christopher Chapman)

A: np-Au (50kx)



B: np-Au (200kx)



C: pl-Au (200kx)

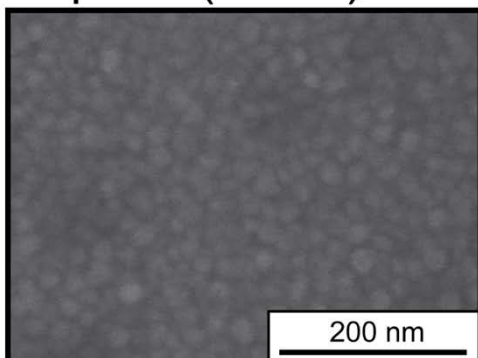
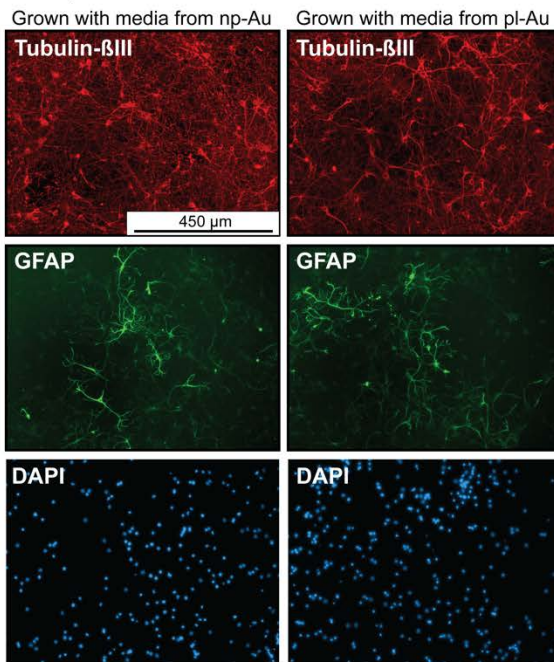
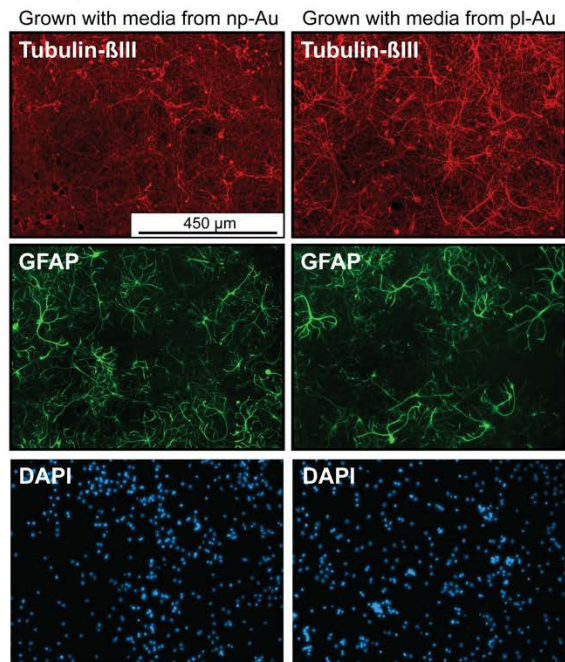
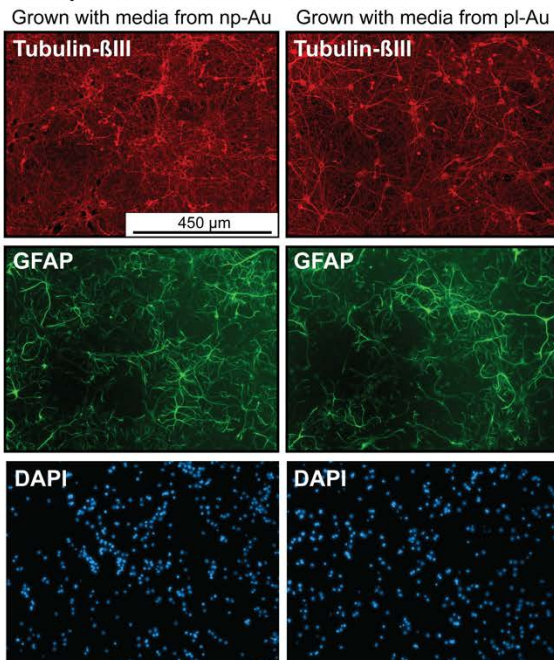


Figure 4 (Christopher Chapman)

A: Day *in vitro* 1 conditioned media:B: Day *in vitro* 7 conditioned media:C: Day *in vitro* 12 conditioned media:

D: Non-conditioned media (Control)

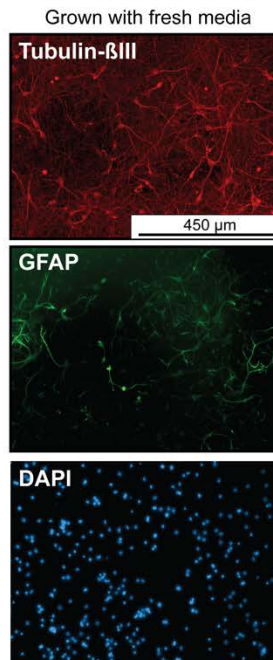
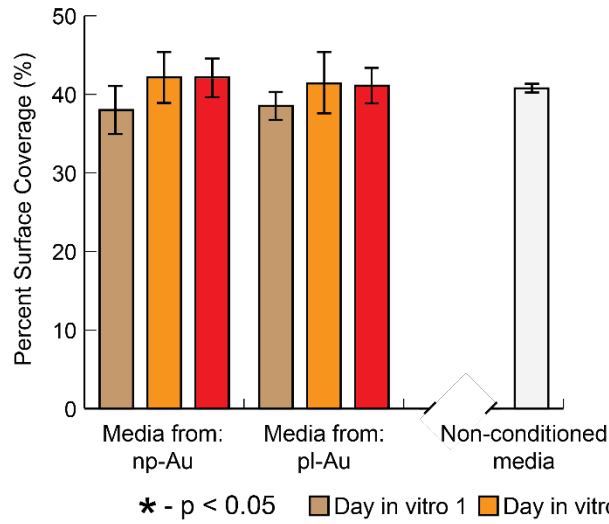
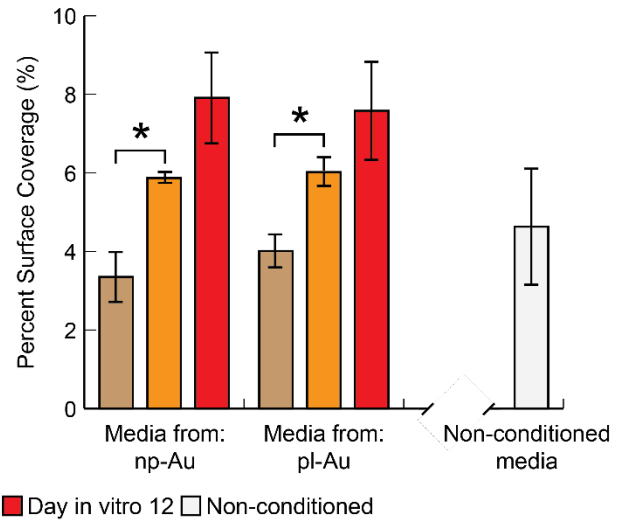


Figure 5 (Christopher Chapman)

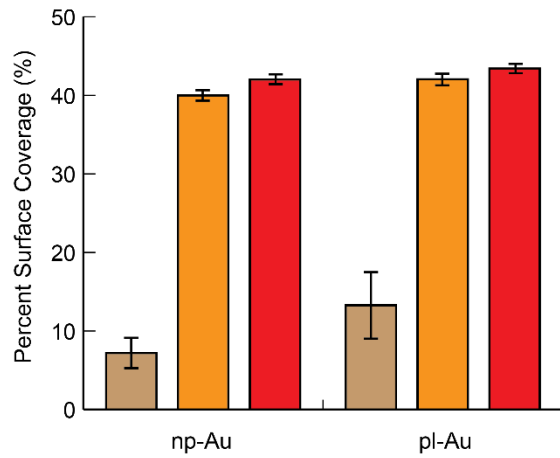
A: Neuron Surface Coverage on TCP at DIV 7



B: Astrocyte Surface Coverage on TCP at DIV 7



C: Neuron Surface Coverage on np-Au and pl-Au Samples



D: Astrocyte Surface Coverage on np-Au and pl-Au Samples

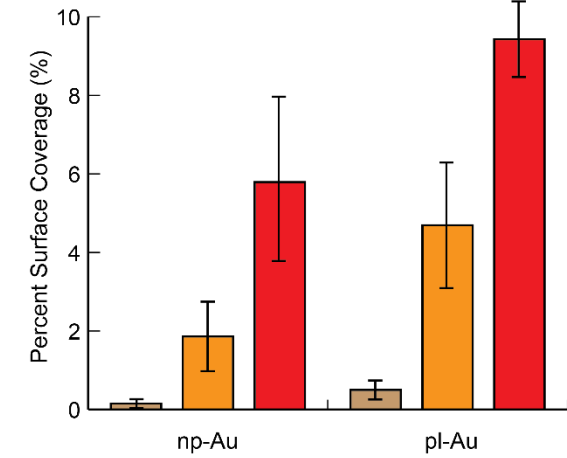


Figure 6 (Christopher Chapman)

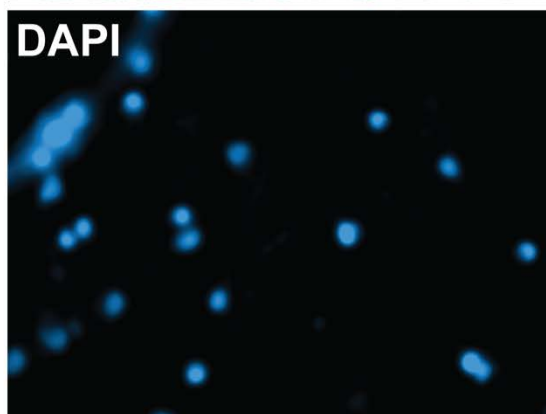
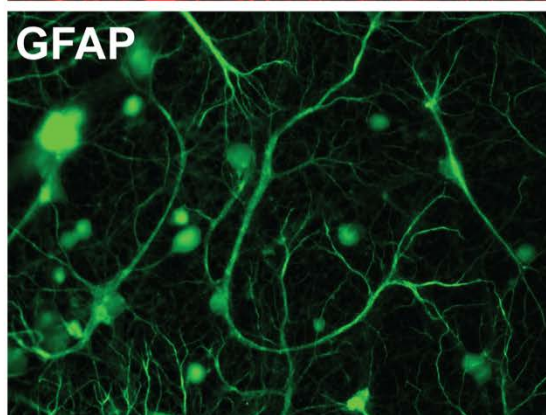
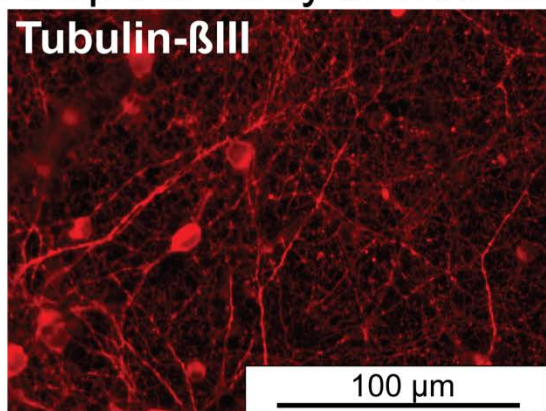
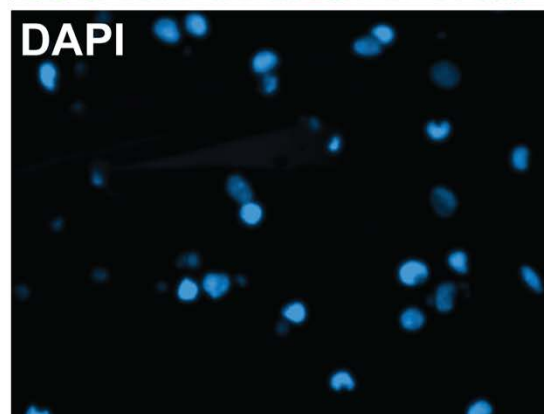
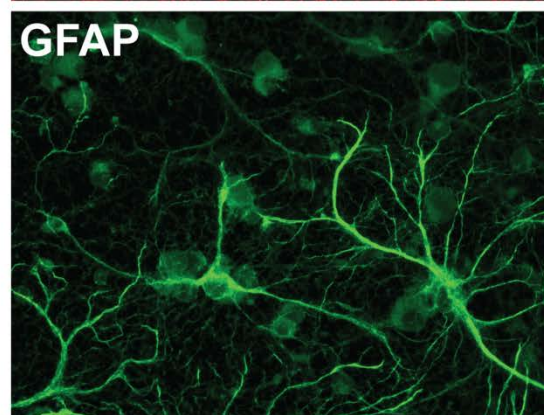
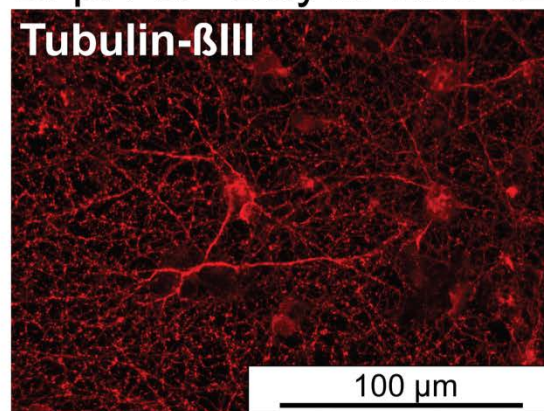
A: np-Au - Day *in vitro* 12B: pl-Au - Day *in vitro* 12

Figure 7 (Christopher Chapman)

